ELSEVIER

Nuclear Physics A 586 (1995) 1–19

NUCLEAR PHYSICS A

Coexistence in even–even Cd nuclei: global structure and local perturbations

K. Heyde [a], J. Jolie [b], H. Lehmann [b], C. De Coster [c], J.L. Wood [d]

[a] *Vakgroep Subatomaire en Stralingsfysica, Institute for Theoretical Physics, Proeftuinstraat 86, B-9000 Gent, Belgium*

[b] *Institut de Physique, Université de Fribourg, Pérolles, CH-1700 Fribourg, Switzerland*

[c] *Vakgroep Subatomaire en Stralingsfysica, Institute for Theoretical Physics, Proeftuinstraat 86, B-9000 Gent, Belgium*

[d] *School of Physics, Georgia Institute of Technology, Atlanta, GA 30332, USA*

Received 15 September 1994

Abstract

The even–even Cd nuclei near neutron number $N = 66$ are indicative of the presence of two rather distinct families of excitations: anharmonic quadrupole vibrations and more deformed intruder particle–hole excitations. We discuss these excitations as mainly coexisting families of states forming the *global* structure of these nuclei. Then, we investigate how *local* large perturbations can cause strong mixing between the two families. The coupling is studied in detail and a particular set of selection rules governing the mixing leads to the introduction of a new basis in order to discuss the interaction between vibrational and intruder excitations. Numerical applications are carried out for ^{112,114}Cd.

1. Introduction

In the study of nuclear structure properties in nuclei with just a few protons (neutrons) away from a closed shell configuration but many valence neutrons (protons), one encounters the characteristics of anharmonic quadrupole vibrational excitations mainly. It has been shown though that in the $Z = 50$ mass region (Cd, Te, ...) [1–11] and, similarly in the $Z = 82$ mass region ([10] and references therein) a number of extra states below the pair gap breaking energy do appear in a systematic way which cannot easily be accommodated in the vibrational picture.

It is precisely the mass regions where a systematic observation of particle–hole (p–h) excitations has been made in the odd-mass nuclei adjacent to the $Z = 50$ (In, Sb) and $Z = 82$ (Tl, Bi) nuclei [11]. These p–h excitations can give rise to deformed

SSDI 0375-9474(94)00721-7

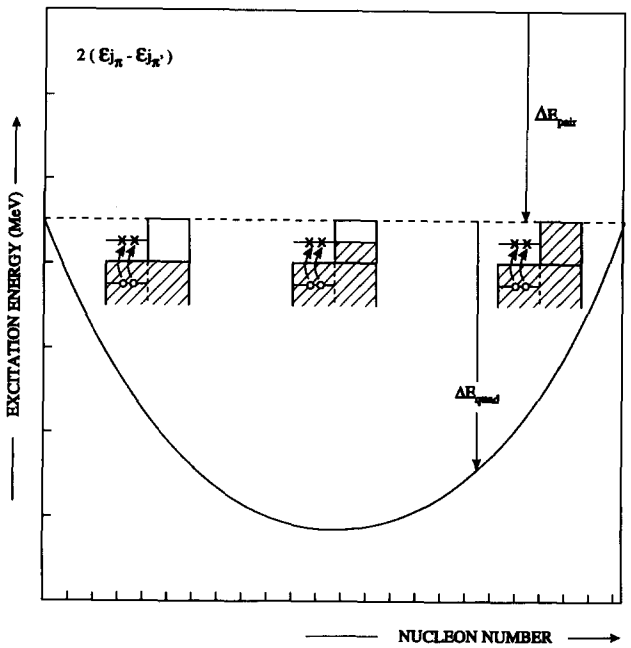

Fig. 1. The variation of the lowest 2p–2h 0^+ intruder configuration over a given mass region, and this as a function of the number of valence nucleons (i.e. neutron numbers for a proton 2p–2h excitation) [10]. Both the pairing energy correction (ΔE_{pair}) as well as the relative binding energy gain due to quadrupole proton–neutron interactions are drawn, albeit in a schematic way. The specific particle configurations are drawn as inserts.

states coexisting with the regular, low-lying excitations. In that spirit, it is quite a small step to suggest the appearance of similar p–h excitations in the even–even nuclei at or near to the closed shells. The most dramatic examples of possible 2p–2h excitations across a major shell closure have been seen in the even–even Pb nuclei [12,13] and in the Pb region (Hg, Pt, Po, ...). Also the Sn region (Sn nuclei [14] and nearby Cd nuclei) are good examples where both vibrational and intruder states do appear. The fact that these intruder p–h excitations can compete in excitation energy with the more regular excitations is mainly due to the large binding energy gain realized within the intruder configuration (2p–2h) originating from the proton–neutron interactions. This behavior can be rather easily derived when using a quadrupole proton–neutron force and shows maximal binding energy gain at the mid-shell configurations (for Sn, Cd, Te near $N = 66$; for Hg, Pb, Po near $N = 104$, ...). In Fig. 1 a schematic illustration of the mass dependence for the lowest 0^+ intruder state is shown.

The question whether no other explanations or descriptions can equally well account for these extra excitations, of course, comes up. There have been attempts made to explain the extra states as resulting from very large anharmonicities in the vibrational model, bringing states from higher phonon multiplets down in energy [4–6,15–17]. Given the fact that most $B(\text{E2})$ values seem to fulfill the harmonic vibrational intensity

and selection rules has been a guide in that respect. There is, however, a problem since large energy anharmonicities will mostly lead to large anharmonicities in the $B(E2)$ values too, and the aim is an understanding of *both* the energies and E2 decay rates within a single framework and thus for *all* states below the pair gap.

Still other explanations have invoked the idea that in coupling the proton and neutron excitations, modes where the different charge components are coupled in a non-symmetric way (mixed-symmetry states within the IBM-formalism [18]) might explain the extra low-lying 2^+ states [7,8]. Even though this approach gives some success for the particular extra 2^+ state, the low-lying 0^+ extra state is missing in the description and the energy dependence of the mixed-symmetry states is difficult to understand [19].

It seems, looking to the large systematic basis on the appearance of intruder p–h bands near closed shells, that only the picture including shape coexistence related to the extra pairs being created relative to the normal states can give a rather consistent and general framework in order to describe the extra states near closed shells [19].

In recent years, the Cd isotopes have received particular interest in testing the above ideas. A variety of techniques encompassing γ-ray spectroscopy, inelastic scattering studies, transfer reactions, ...have allowed to establish level schemes as complete as possible for a large chain of Cd nuclei [1–8,20–22] with rather compelling evidence for 0^+ intruder states near the $N = 66$ mid-shell region and, in ^{110,112}Cd, with intruder bands extending to rather high excitation energy and high-spin values.

The aim of the present paper is (i) to show that a global structure is present in the Cd nuclei comprising both the set of anharmonic quadrupole vibrational excitations and the intruder bands (Section 2.1) and, (ii) to indicate evidence that only very local perturbations will mix the two families at well defined spin values. The precise meaning of the terms "global" and "local" are defined in Ref. [19]. We investigate a new basis which incorporates most of the effects due to the presence of rather selective mixing related to underlying similarities (a common $O(5)$ subgroup in the IBM group chains) [23] between the vibrational and intruder excitations.

The formulation makes use of the IBM algebraic structure [18] where 2p–2h excitations can be considered as two extra bosons. The configuration mixing picture, as worked out originally by Duval and Barrett, is thereby used [24]. Even though a number of numerical studies of intruder excitations concentrating on the Cd nuclei have been carried out [3,25–30], we shall concentrate on (i) the underlying mechanism causing the coupling between the vibrational and intruder bands to be so selective [23,19], and, (ii) the possibility of having intruder analog multiplets surviving to a large extent in these Cd nuclei [31] making up for the global, rather simple structure of these Cd nuclei.

We also point out that a possibility exists to bridge the gap between *on one hand* calculations using the IBM configuration mixing and starting from a basis that implies *strong mixing* for certain states (0^+ states) and, *on the other hand*, attempts to describe all observed E2 properties using rather an *unmixed picture* of anharmonic quadrupole vibrations serving as the physical basis.

2. Coexistence in the even–even Cd nuclei: global properties and local perturbations

In the present section, we try to describe the main features of *all* excited states up to the energy where the multitude of more complex broken-pair shell-model configurations appear in the spectra. Even in this region, a number of collective bands can be observed to rather high spin values [1–3].

We first concentrate on the main structures: the Cd nuclei are still approximately behaving like anharmonic quadrupole vibrators, at first instance. The presence of a number of extra states near the two-phonon energy, and a band associated with a more deformed, intrinsic structure is also quite clear [1–8]. These two features: anharmonic quadrupole vibrational excitations completed with intruder bands makes up for the *global* nuclear structure properties. Whenever states of these different families come close together, large mixing of the wave functions should inevitably show up: these perturbations will result in modifications in the electromagnetic decay properties of the independent subsystems [32]. We call these the *local* perturbations, following Ref. [19].

It is our aim to describe both global and local properties as correct as possible.

2.1. Global symmetry properties

One has observed that a description of *all* low-lying levels in the even–even Cd nuclei making use of anharmonic quadrupole vibrational excitations is not easily possible. Introduction of various anharmonic corrections to the purely harmonic vibrator can stretch the region of validity of the basic quadrupole vibrational picture but it remains rather difficult to describe both (i) the precise energy of the various members and (ii) the E2 transition rates [5,6,15–17].

Making use of the U(5) limit of the interacting boson model [18] and starting from the hamiltonian in this chain, which results into the energy expression

$$E(n_d, v, L) = \epsilon n_d + \alpha n_d(n_d + 4) + \beta v(v + 3) + \gamma L(L + 1), \tag{1}$$

where ϵ, α, β and γ denote the strengths for the various Casimir operators (linear U(5), quadratic U(5), quadratic O(5) and quadratic O(3), respectively); fits have been made for various even–even Cd nuclei (see Fig. 2) [3,19,33,34]. Even though these fits give a rather good description of a large part of the low-lying states, a large number of levels are still missing to complete the global structure as observed in the even–even Cd nuclei.

The additionally observed low-lying states could be interpreted as intruder excitations, in the light of the observation of low-lying intruder excitations appearing systematically in both odd-mass In ($1/2^+$, $3/2^+$, ...); Sb ($9/2^+$, $11/2^+$, ...) [11] as well as in the even–even Sn nuclei (0^+, 2^+, 4^+, ... band) [10] preferentially near the neutron mid-shell $N = 66$ position. Microscopically, they are understood to be 4h–2p excitations that acquire a particular low energy through the increased proton–neutron binding energy, relative to the regular 2h configurations. This idea has been developed in a systematic way and has been amply illustrated to persist experimentally in many more mass re-

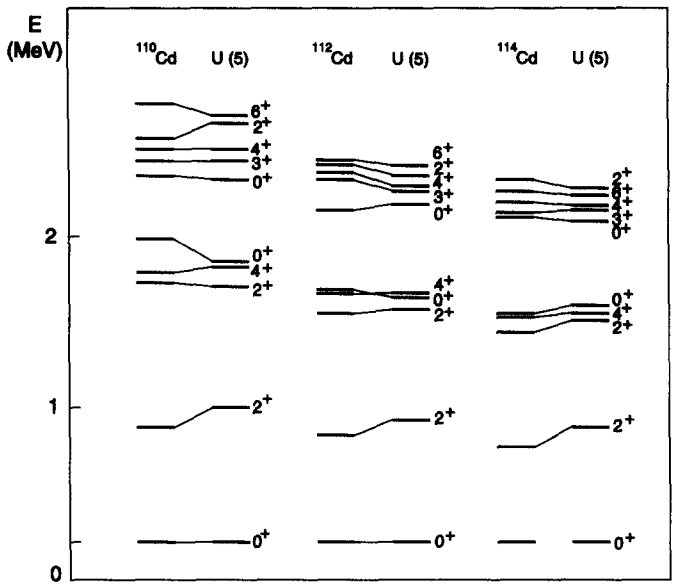

Fig. 2. Comparison between the theoretical U(5) description of excitations in ^{110,112,114}Cd with the anharmonic quadrupole vibrational part of the experimental spectrum [19].

gions [10]. In completing the family of anharmonic quadrupole vibrational excitations with the intruder excitations, one might well reach a global description in the even–even Cd nuclei.

Following the suggestion of a possible classification of the intruder bands as members of intruder analog multiplets [31] where particle and hole bosons are considered as spin $+1/2$ and $-1/2$ projections of intruder spin $1/2$ objects, a connection between

$$nh \leftrightarrow (n-2)h-2p \leftrightarrow (n-4)h-4p \leftrightarrow \ldots np \tag{2}$$

configurations could be made. In such a description the intruder 4h–2p states in the even–even Cd nuclei would be members of a $I = 3/2$ multiplet (with $I_z = -1/2$) and thus should resemble the ground-state bands in the $I = 3/2$, $I_z = -3/2$ Ru even–even nuclei [3,31,34]. That this is rather well the case is shown in Fig. 3. As the Ru isotopes are γ-unstable nuclei, the intruder band should be approximately described by the O(6) limit of the IBM [18], with corresponding energy formula

$$E(\sigma,\tau,L) = \alpha'\sigma(\sigma+4) + \beta'\tau(\tau+3) + \gamma' L(L+1)\,, \tag{3}$$

or, alternatively,

$$E(\sigma,\tau,L) = \alpha''(N-\sigma)(N+\sigma+4) + \beta''\tau(\tau+3) + \gamma'' L(L+1)\,, \tag{4}$$

where α', β', γ' are the strengths of the quadratic O(6), O(5) and O(3) Casimir operators, respectively. The α'', β'', γ'' strengths are related to α', β', γ' as discussed e.g. by Casten and Warner [35].

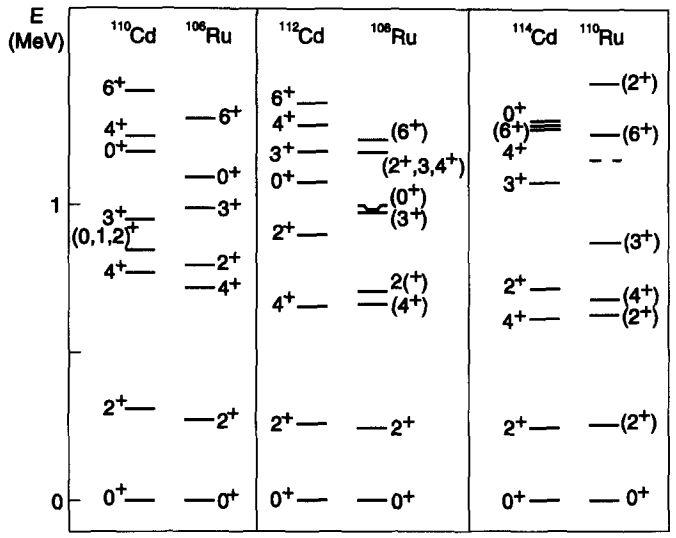

Fig. 3. Comparison of the intruder multiplet structure (2p–4h configuration) in the ^{110,112,114}Cd nuclei (normalized to the lowest 0^+ intruder state) with the corresponding ground-state bands (6 hole configurations) in the even–even ^{106,108,110}Ru nuclei [19].

Putting the formulae 1 and 3 (or 4) together, one obtains a rather good description of *all* states and can make up for a global picture to discuss the even–even Cd nuclei.

2.2. *Mixing: strong versus weak-mixing*

It is clear that the two families (U(5)-like and O(6)-like or, anharmonic quadrupole vibrations and the intruder bands) will most probably mix whenever equal J^π states come close together. It was shown, using a method developed by Duval and Barrett [24], how such an intruder band can interact with the regular bands. Starting from configuration mixing calculations taking into account both the two-hole ($\bar{N}_\pi = 1$) and 4h–2p ($\bar{N}_\pi = 3$) boson states, as well as the relative energy difference caused by the energy needed to create an additional 2p–2h pair, rather detailed calculations in the Cd region and other mass regions could be carried out [25–30]. A general mixing hamiltonian, determined within the IBM formalism, connects the N to $N+2$ model space by creating two more pairs (a 2p–2h excitation). In the sd-boson model, one could either do this creating two more s bosons or two more d bosons, so the coupling hamiltonian reads [1]

$$H_{\mathrm{mix}} = \alpha \left(s^+ s^+ + \mathrm{h.c.}\right)^{(0)} + \beta \left(d^+ d^+ + \mathrm{h.c.}\right)^{(0)} . \tag{5}$$

[1] Here, no distinction between particle and hole-like bosons nor between proton and neutron bosons is made. So, one should in the more general case use $s^+_{\mathrm{p},\rho}$, $d^+_{\mathrm{p},\rho}$ and $s^+_{\mathrm{h},\rho}$, $d^+_{\mathrm{h},\rho}$ (p: particle, h: hole; $\rho \equiv \pi, \nu$ proton, neutron) bosons. This distinction can be made in making the intruder analog multiplet structure appear more precisely [31].

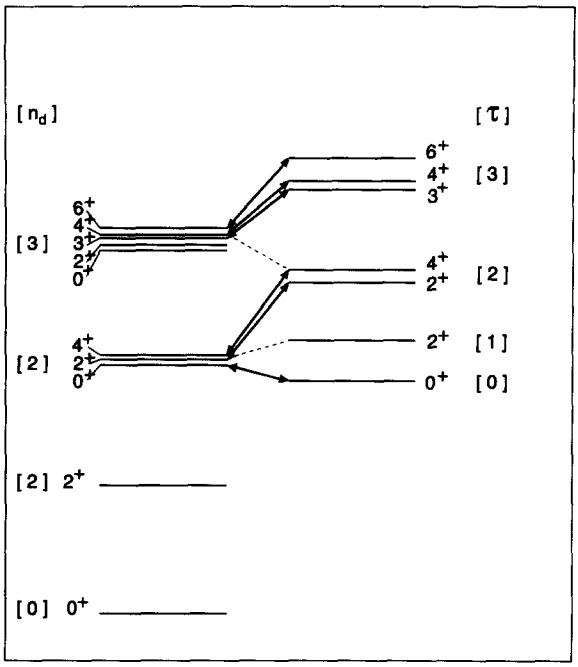

Fig. 4. The coupling between a U(5) and intruder O(6) spectrum (scale arbitrary but drawn after the typical situation as observed in the even–even Cd nuclei). The quantum numbers n_d (in the U(5) limit) and τ (for the O(6) limit) are denoted. Forbidden matrix elements are denoted by the dotted lines [23,19].

In terms of the intruder spin this means that $|\Delta I| = 1$ couplings are possible and, using the sd-boson model structure that $\Delta n_d = 0, \pm 2$ coupling terms will result.

The detailed, numerical studies of the mixing between the N and $N+2$ configuration spaces carried out within the proton–neutron IBM (IBM-2) leads to the introduction of quite some extra parameters [25–30]. Their determination is constrained by the simultaneous description of many isotopes [26,30] and by microscopic arguments [30,32]. Here, we first look to the more general features the above coupling hamiltonian can create. To highlight the coupling effects, we use the U(5)–O(6) model [3], which allows an analytic treatment of shape coexistence [33].

2.2.1. Mixing the pure U(5) and O(6) symmetries

In Fig. 4 we indicate in a schematic way (adjusted to the more realistic cases of ^{110,112,114}Cd) the relative positions of the lowest U(5) and O(6) multiplet members. Even though, near the two-phonon 0^+, 2^+, 4^+ $n_d = 2$ states the lowest O(6) 0^+, 2^+ states show up, the coupling hamiltonian imposes certain selection criteria [3,19], which are related to the common O(5) subgroup [23].

Trivially, the mixing hamiltonian only connects states with $\Delta n_d = 0, \pm 2$. This selection rule is, however, not the only one that affects the mixing. To illustrate this, we can consider the intruder states to be described by the O(6) symmetry. Then, one can

expand a pure O(6) state, characterized by given $N+2$, σ, τ, L values, into the U(5) basis, i.e.

$$|[N+2],\sigma,\tau,L\rangle = \sum_{n_d} a_{n_d}^{N+2,\sigma,\tau=v} |[N+2],n_d,v,L\rangle \ , \tag{6}$$

where N refers to the number of bosons in the normal configuration and the sum over n_d goes as:

$$n_d = \tau, \tau+2, \tau+4, \ldots \leqslant N+2. \tag{7}$$

This decomposition, studied in detail in Refs. [23,19], forbids any coupling of U(5) and O(6) states, even when they are degenerate, if

$$\tau - n_d = \text{odd}. \tag{8}$$

This condition (8) allows strong mixing between 0_2^+ and 0_3^+ states but no mixing between 2_2^+ and 2_3^+ states. This behavior was very recently observed in ^{112}Cd by Hertenberger et al. [36] in (p,p') and (d,d') experiments. The mixing conditions can be defined in a more succinct way by noting that the mixing hamiltonian (5) can be rewritten as an O(5) scalar operator implying the even more stringent condition $v = \tau$ [19]. Thus one obtains the selection rules on the mixing by

$$\Delta L = 0; \qquad \Delta n_d = 0, \pm 2; \qquad v = \tau, \tag{9}$$

if the intruder states are described by O(6) and the regular states by U(5). In Fig. 4 the states which, according to the above selection rules, can mix are linked by a thick arrow, forbidden couplings with dotted lines. One has to keep in mind that coupling matrix elements are quite small and 100 keV is almost an upper limit. In the light of typical energy separations e.g. for the 4_1^+ and 4_2^+ states, 6_1^+ and 6_2^+ states, even allowed coupling terms will give rise to rather small mixing effects.

It is this selection mechanism which makes that the global structure remains intact up to rather high spin states, and that only a few cases (0_2^+–0_3^+ as the most dominant coupling) give rise to locally strong deviations from coexisting band structures.

2.2.2. The choice of a basis

In practice, when trying to describe the even–even Cd nuclei, one goes beyond the U(5) and O(6) basis states. Realistic IBM-2 hamiltonians, as discussed before [2,10,25–27,29,30,32,34,36], however do preserve in part the selective mixing when inspecting the obtained wave functions.

Knowing that the major coupling for the region $E_x \tilde{<} 1.5$ MeV is mainly situated in the 0_2^+–0_3^+ channel which has as consequence an important modification of the E2 transition rates, we propose to take into account this observation by carrying out a *two-step diagonalization* of the mixing hamiltonian:

(i) The realistic model spaces describing the regular (proton two-hole configurations) and the intruder (proton four-hole two-particle configurations) excitations are ob-

tained according to the Duval, Barrett method [24] and denoted by $|J_i^\pi; \bar{N}_\pi = 1\rangle$ and $|J_j^\pi; \bar{N}_\pi = 3\rangle$, respectively.

(ii) Considering the major effects of $H_{\rm mix}$, Eq. (5), as outlined in the analytic O(6)–U(5) coupling model [23,34], to be preserved, a strong coupling between the 0_2^+ and 0_3^+ states and only weak coupling between the 2_2^+–2_3^+ and 4_1^+–4_2^+ levels occur. Then, the matrix U carrying out the transformation from the basis $|J_i^\pi; \bar{N}_\pi = 1\rangle$, $|J_j^\pi; \bar{N}_\pi = 3\rangle$ to the actual eigenstates can be split into a part $U^{(s)}$ (s: strong mixing, following the O(6)–U(5) coupling model) followed by a part $U^{(w)}$ (w: weak mixing part):

$$U = U^{(w)} U^{(s)} . \tag{10}$$

The transformation

$$U^{(s)} \begin{pmatrix} |J_i^\pi; \bar{N}_\pi = 1\rangle \\ |J_j^\pi; \bar{N}_\pi = 3\rangle \end{pmatrix} , \tag{11}$$

results into the intermediate (called *new*) basis as approximate eigenstates to the full problem and where the remaining, more detailed mixing effects are diagonalized by $U^{(w)}$.

The matrix $U^{(s)}$ is determined by inspecting the major effects caused by $H_{\rm mix}$ on the final wave functions for a given Cd nucleus. Thus, the structure and amplitudes can change somewhat in proceeding through the whole series of even–even Cd nuclei in the mid-shell (around $N = 66$) region. For ^{114}Cd we have chosen the new basis as

$$\begin{aligned}
|0_1^+\rangle &= |0_1^+; \bar{N}_\pi = 1\rangle , \\
|0_2^+\rangle &= \frac{1}{\sqrt{2}} |0_2^+; \bar{N}_\pi = 1\rangle + \frac{1}{\sqrt{2}} |0_1^+; \bar{N}_\pi = 3\rangle , \\
|0_3^+\rangle &= \frac{1}{\sqrt{2}} |0_2^+; \bar{N}_\pi = 1\rangle - \frac{1}{\sqrt{2}} |0_1^+; \bar{N}_\pi = 3\rangle , \\
|2_1^+\rangle &= \sqrt{1-\epsilon^2}\, |2_1^+; \bar{N}_\pi = 1\rangle + \epsilon |2_1^+; \bar{N}_\pi = 3\rangle , \\
|2_2^+\rangle &= \gamma |2_2^+; \bar{N}_\pi = 1\rangle + \delta |2_1^+; \bar{N}_\pi = 3\rangle , \\
|2_3^+\rangle &= -\delta |2_2^+; \bar{N}_\pi = 1\rangle + \gamma |2_1^+; \bar{N}_\pi = 3\rangle , \\
|4_1^+\rangle &= \gamma' |4_1^+; \bar{N}_\pi = 1\rangle + \delta' |4_1^+; \bar{N}_\pi = 3\rangle , \\
|4_2^+\rangle &= -\delta' |4_1^+; \bar{N}_\pi = 1\rangle + \gamma' |4_1^+; \bar{N}_\pi = 3\rangle ,
\end{aligned} \tag{12}$$

with $\gamma = \gamma' = 0.95$, $\delta = \delta' = 0.30$ and $\epsilon = -0.12$. The small, but non-zero value of ϵ already takes into account in the new basis some small intruder state mixing effects in the 2_1^+ state (mainly one-quadrupole phonon $\bar{N}_\pi = 1$ state) which will prove to be important in determining the effective E2 operator acting in this new basis. We also allow by γ and δ a slight perturbation compared to the more stringent U(5)–O(6) model in which the $|2_2^+\rangle$ and $|2_3^+\rangle$ do not mix [23].

This intermediate basis should approximate the experimental situation already quite well and will determine new effective E2 matrix elements through the relation

Table 1
E2 reduced matrix elements in the unperturbed "vibrational" ($\bar{N}_\pi = 1$) and "intruder" ($\bar{N}_\pi = 3$) basis (units $e{\cdot}\mathrm{fm}^2$)

$\bar{N}_\pi = 1$		$\bar{N}_\pi = 3$	
$\langle 2_1^+ \|\| M(\mathrm{E2}) \|\| 0_1^+ \rangle$	−70	$\langle 2_1^+ \|\| M(\mathrm{E2}) \|\| 0_1^+ \rangle$	126
$\langle 2_1^+ \|\| M(\mathrm{E2}) \|\| 0_2^+ \rangle$	−33	$\langle 2_1^+ \|\| M(\mathrm{E2}) \|\| 2_1^+ \rangle$	90
$\langle 2_1^+ \|\| M(\mathrm{E2}) \|\| 2_1^+ \rangle$	−37	$\langle 2_1^+ \|\| M(\mathrm{E2}) \|\| 4_1^+ \rangle$	200
$\langle 2_2^+ \|\| M(\mathrm{E2}) \|\| 0_2^+ \rangle$	−28	$\langle 4_1^+ \|\| M(\mathrm{E2}) \|\| 4_1^+ \rangle$	80
$\langle 2_1^+ \|\| M(\mathrm{E2}) \|\| 2_2^+ \rangle$	−83		
$\langle 2_2^+ \|\| M(\mathrm{E2}) \|\| 2_2^+ \rangle$	19		
$\langle 2_1^+ \|\| M(\mathrm{E2}) \|\| 4_1^+ \rangle$	−120		
$\langle 2_2^+ \|\| M(\mathrm{E2}) \|\| 4_1^+ \rangle$	−20		
$\langle 4_1^+ \|\| M(\mathrm{E2}) \|\| 4_1^+ \rangle$	−60		

$$\langle J_i^\pi \|\| M(\mathrm{E2}) \| J_f^\pi \rangle = \sum_{\substack{j,\bar{N}_\pi \\ k,\bar{N}_\pi}} U^{(s)} \left(J_i^\pi ; j\bar{N}_\pi \right) U^{(s)} \left(J_f^\pi ; k\bar{N}_\pi \right) \langle J_j^\pi ; \bar{N}_\pi \|\| M(\mathrm{E2}) \|\| J_k^\pi ; \bar{N}_\pi \rangle, \tag{13}$$

where the $U^{(s)}$ elements are nothing but the coefficients as given by the wave functions of Eq. (12). From the knowledge of the elementary matrix elements $\langle J_j^\pi ; \bar{N}_\pi = 1 \|\| M(\mathrm{E2}) \|\| J_k^\pi ; \bar{N}_\pi = 1 \rangle$ and the analogous matrix elements but now with $\bar{N}_\pi = 3$, one gets simple expressions. In Table 1, we present these elementary "uncoupled" $\bar{N}_\pi = 1$ and $\bar{N}_\pi = 3$ matrix elements (in units $e{\cdot}\mathrm{fm}^2$). The values are determined according to the IBM-2 calculation of Ref. [30] for ^{114}Cd using *all the parameters as fixed in that study*. In Table 2, we then show for the various transitions, both the "uncoupled" value, the contributions to Eq. (13) from the $\bar{N}_\pi = 1$ part (called vibrational), from the $\bar{N}_\pi = 3$ part (intruder) as well as the total value (in units $e{\cdot}\mathrm{fm}^2$). Thereby, new effective charges are defined and it is interesting to see what the major changes induced to the "uncoupled" scheme will be. We illustrate these results in Fig. 5. At first glance, almost no changes occur except for

(i) a coupling of the otherwise uncoupled 2_3^+ state, decaying to the lower-lying 2_2^+,
(ii) the strong $0_3^+ \rightarrow 2_2^+$ E2 transition.

In this intermediate basis, one has lost the pure interpretation of a two-phonon quadrupole 0^+ state and an intruder 0^+ state through the perfect $1/\sqrt{2}$, $1/\sqrt{2}$ linear combination. Almost the same linear combination was obtained with the coupling model in Ref. [34]. This intermediate basis comes already quite close to explaining the experimental situation. Therefore, the remaining modifications (in general) to E2 transitions and energy shifts will be rather small. In Table 2 we also give the experimental E2 matrix elements as derived by Fahlander et al. [6]. A comparison of these matrix elements and the newly derived, effective E2 matrix elements is interesting. One observes that

(i) if a certain E2 matrix element arises from a transition allowed in the uncoupled picture (column 2 of Table 2), the final theoretical value (column 5) never deviates

Table 2
The results for the effective E2 matrix elements after applying that part of the diagonalization, called $U^{(s)}$ (Eq. (11)). Both the uncoupled, the total vibrational ($\tilde{N}_\pi = 1$) and intruder ($\tilde{N}_\pi = 3$) parts to the E2 matrix element are given. The total value is given (all in units $e\cdot\mathrm{fm}^2$) as well as the E2 matrix elements deduced from experiment by Fahlander et al. [6] (column Exp.). The present table is used to construct the right-hand part in Fig. 5

$J_i^\pi \to J_f^\pi$	Uncoupled	Vibrational	Intruder	Total	Exp. [a]
$2_1^+ \to 0_1^+$	−70(V)	−70	0	−70	71.4
$0_2^+ \to 2_1^+$	0	−23	−11	−34	30.0
$2_2^+ \to 0_1^+$	0	0	0	0	9.1
$\to 2_1^+$	−83(V)	−79	−3	−82	60.6 [b]
$\to 0_2^+$	0	−19	31	12	−17.0
$4_1^+ \to 2_1^+$	−120(V)	−114	−7	−121	135.0
$\to 2_2^+$	−20(V)	−18	18	0	−35.0
$0_3^+ \to 2_1^+$	−33(V)	−23	11	−12	0.30
$\to 2_2^+$	−28(V)	−18	−31	−49	67.0 [b]
$2_3^+ \to 0_1^+$	0	0	0	0	7.30
$\to 2_1^+$	0	25	−10	15	2.50
$\to 0_2^+$	126(I)	6	84	90	103.0 [b]
$\to 4_1^+$	0	6	57	63	86.0 [b]
$\to 2_2^+$	0	5	−26	−21	73.0 [b]
$\to 0_3^+$	0	6	−84	−78	33.0
$4_2^+ \to 2_1^+$	0	36	−23	13	11.0
$\to 2_2^+$	0	6	57	63	97.0
$\to 2_3^+$	200(I)	2	−180	−178	185.0
$\to 4_1^+$	0	17	23	40	61.0
$2_1^+ \to 2_1^+$	−37(V)	−37	1	−36	−36.0
$2_2^+ \to 2_2^+$	19(V)	17	1	18	92.0
$2_3^+ \to 2_3^+$	90(I)	2	81	83	29.0
$4_1^+ \to 4_1^+$	−60(V)	−54	7	−47	−95

[a] Ref. [6] Fahlander et al. data.
[b] These values are rescaled from Ref. [6] using the branching ratios determined and discussed in Ref. [5].

much from the uncoupled value and comes quite close to the experimental matrix elements (column 6), except for the $4_1^+ \to 2_2^+$ and $0_3^+ \to 2_1^+$ transitions. In both cases, strong destructive interference between the vibrational and intruder part shows up and even minor modifications of the small factors δ and ϵ can change these values in a decisive way (changing ϵ from −0.12 to −0.25 would give almost exact cancellation for the $0_3^+ \to 2_1^+$, E2 matrix element). So, the intermediate or new basis cannot produce *stable* numbers for those transitions.

(ii) for those E2 transitions that are forbidden in the uncoupled basis (value of 0 in column 2), the new basis results in almost *all* cases ($0_2^+ \to 2_1^+$; $2_2^+ \to 0_2^+$; $2_3^+ \to 2_1^+, 4_1^+, 2_2^+, 0_3^+$; $4_2^+ \to 2_1^+, 2_2^+, 4_1^+$) in a serious improvement and approaches

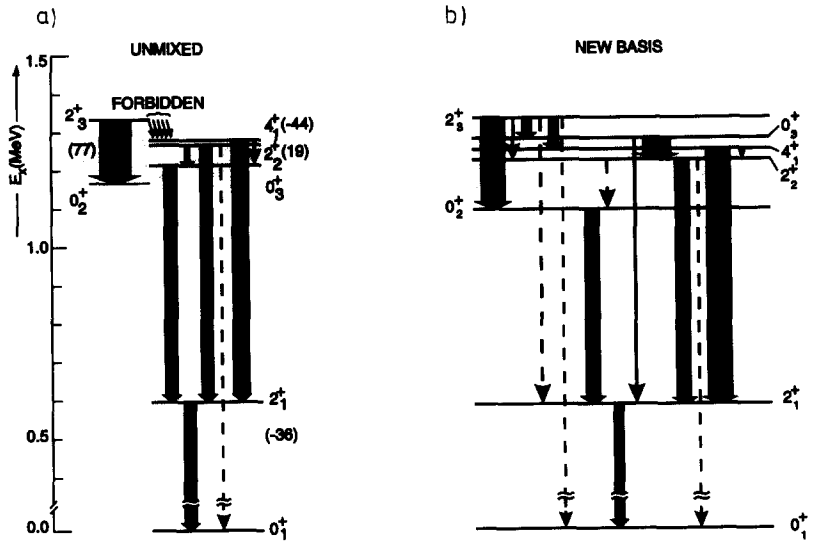

Fig. 5. (a) The quadrupole vibrational ($\tilde{N}_\pi = 1$) and intruder ($\tilde{N}_\pi = 3$) B(E2) values in ^{114}Cd for an uncoupled situation. The widths of the arrows have been normalized to the $B(\mathrm{E2}; 2_1^+ \rightarrow 0_1^+)$ value ($\simeq 1000\ e^2\mathrm{fm}^4$). Values between brackets denote the diagonal matrix elements $\langle J_i^\pi || M(\mathrm{E2}) || J_i^\pi \rangle$ for the 2_1^+ and 4_1^+ states also in units $e{\cdot}\mathrm{fm}^2$. Forbidden transitions are indicated (dashed lines). (b) The same as for (a) but now using the wave functions obtained using the basis (Eq. (12)) after the transformation $U^{(s)}$. The new, effective B(E2) values and E2 diagonal matrix elements are drawn with the convention described under (a).

the experimental E2 matrix elements. Here, the action of the remaining weak-mixing transformation $U^{(w)}$ improves the comparison of the theoretical E2 matrix elements with the numbers of Fahlander et al. [6].

At this point, we like to comment on the studies by Casten et al. [5] and Fahlander et al. [6] trying, in part, to constrain the structure of Cd nuclei to that of an anharmonic quadrupole vibrator. It is indeed very close to reality that, looking to E2 transitions, one might make the choice of a "physical" basis that relates to a strongly perturbed quadrupole vibrator in the energies, keeping the E2 rates rather well intact according to the original E2 vibrational intensity and selection rules. One could say that Casten et al. [5] and Fahlander et al. [6] have somehow "chosen" the intermediate basis (see our Eqs. (12)) to work with. This becomes even more convincing when comparing in detail the E2 matrix elements as deduced by Fahlander et al. [6] with the effective E2 matrix elements as derived in the new, intermediate basis (see our Eqs. (12)). It seems that the selective O(6)–U(5) mixing mechanism modifies the original, uncoupled basis of $|J_i^\pi ; \tilde{N}_\pi = 1\rangle$ and $|J_j^\pi ; \tilde{N}_\pi = 3\rangle$ into a new basis that approaches the observed situation already to a good degree.

So, the resulting outcome is overall a global structure obtained by having the quadrupole anharmonic spectrum (mainly U(5)) and the intruder bands (mainly O(6) symmetry) put together with, a particularly strong local perturbation at the level of the

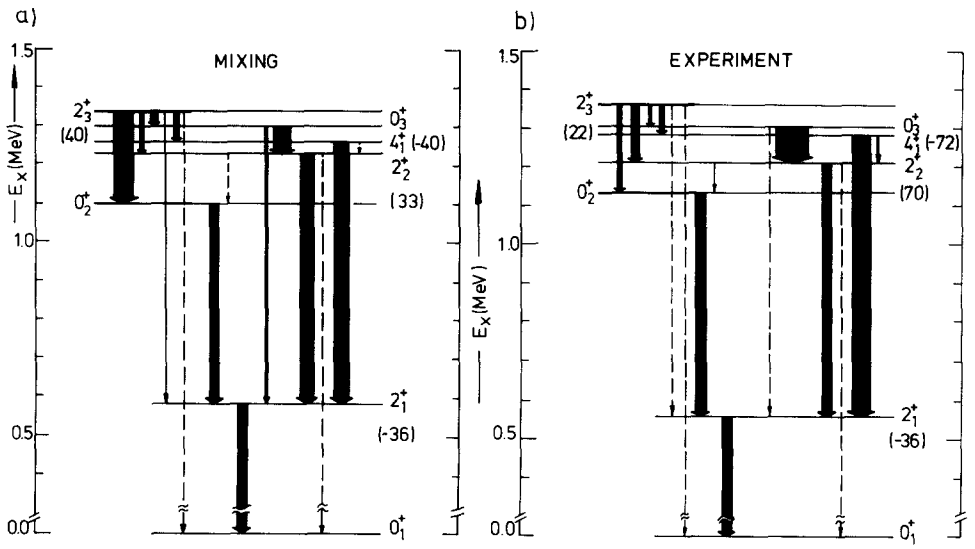

Fig. 6. (a) Same as in Fig. 5a but now for the full diagonalization in ^{114}Cd. (b) Same as in Fig. 5b but now presenting the experimental values in ^{114}Cd.

$\bar{N}_\pi = 1$, 0_2^+ two-phonon and $\bar{N}_\pi = 3$, 0_1^+ lowest intruder state.

2.2.3. *Detailed results for ^{114}Cd*

In order to carry out the full diagonalization one still needs the part $U^{(w)}$ that takes care of the remaining mixing parts, and so a *weak-mixing* in the new, intermediate basis inevitably results. The part $U^{(w)}$ is given by the expression

$$U^{(w)} = U U^{-1(s)}, \tag{14}$$

and has been derived for the case of ^{114}Cd [30]. For the detailed calculation of ^{114}Cd, *all* parameters (hamiltonian, E2 boson effective charges, ...) are identical with the ones used in Ref. [30] with the choice $\epsilon(\bar{N}_\pi = 3) = 0.32$ (see Fig. 6). Before discussing the final E2 pattern (and energies) we give, in Table 3, parts of the $U^{(w)}$ matrices for the 0^+ and 2^+ states. Here, it immediately becomes clear that the maximal mixing between the $|0_2^+, \bar{N}_\pi = 1\rangle$ (quadrupole two-phonon state) and the $|0_1^+, \bar{N}_\pi = 3\rangle$ (lowest 0^+ intruder state) has been transformed away, indicating only very weak mixing with the 0_1^+ state. For the 2^+ state, the lowest part of $U^{(w)}$ shows the same effects and even the small mixing amplitude ($\delta = 0.3$) is transformed away in the final step to almost zero (see the non-diagonal (2,3) and (3,2) elements).

The detailed results concerning B(E2) values are presented in Table 4 where besides the data (column 2), the B(E2) values for both the unmixed ($\alpha = \beta = 0$; column 3) and optimally mixed ($\alpha = \beta = 0.08$, column 4) as well as the values obtained by Délèze et al. [2] for the same nucleus ^{114}Cd, are presented. In order to give an impression on the sensitivity of the B(E2) values to the mixing strengths α and β (see Eq. (5)),

Table 3
(a) The two-step procedure with (i) $U^{(s)}$ and the corresponding basis in the upper part and, (ii) the weak-mixing transformation matrix $U^{(w)}$ now acting on the *new* basis of 0^+ states. Only the lower 3 rows and columns are given here. (b) Same caption as part (a) but now for the 2^+ level

(a)

$$\begin{bmatrix} 1 & 0 & 0 & \cdots \\ 0 & \frac{1}{\sqrt{2}} & \frac{1}{\sqrt{2}} & \cdots \\ 0 & \frac{1}{\sqrt{2}} & -\frac{1}{\sqrt{2}} & \cdots \\ \vdots & \vdots & \vdots & \end{bmatrix} \begin{bmatrix} |0_1^+;\ \bar{N}_\pi = 1\rangle \\ |0_2^+;\ \bar{N}_\pi = 1\rangle \\ |0_1^+;\ \bar{N}_\pi = 3\rangle \\ \vdots \end{bmatrix}$$

$$\begin{bmatrix} 0.9963 & 0.0543 & -0.0459 & \cdots \\ -0.0578 & 0.9925 & -0.0817 & \cdots \\ -0.0405 & -0.0826 & -0.9896 & \cdots \\ \vdots & \vdots & \vdots & \end{bmatrix} \begin{bmatrix} |0_1^+\rangle \\ |0_2^+\rangle \\ |0_3^+\rangle \\ \vdots \end{bmatrix}$$

(b)

$$\begin{bmatrix} 1 & 0 & -0.12 & \cdots \\ 0 & 0.95 & 0.30 & \cdots \\ 0 & -0.30 & 0.95 & \cdots \\ \vdots & \vdots & \vdots & \end{bmatrix} \begin{bmatrix} |2_1^+;\ \bar{N}_\pi = 1\rangle \\ |2_2^+;\ \bar{N}_\pi = 1\rangle \\ |2_1^+;\ \bar{N}_\pi = 3\rangle \\ \vdots \end{bmatrix}$$

$$\begin{bmatrix} 0.997 & 0.0424 & 0.1124 & \cdots \\ 0.030 & 0.9762 & -0.0292 & \cdots \\ -0.026 & 0.0534 & 0.9740 & \cdots \\ \vdots & \vdots & \vdots & \end{bmatrix} \begin{bmatrix} |2_1^+\rangle \\ |2_2^+\rangle \\ |2_3^+\rangle \\ \vdots \end{bmatrix}$$

we have studied the variation of a large number of E2 transitions and illustrated this in Figs. 7a, b and c. As a general conclusion, it shows up that only minor changes result for a 10–15% variation of these coupling strengths.

In comparing the results of Tables 2 and 4, it is clear that the calculation using the intermediate basis, determined via the transformation $U^{(s)}$, gives already (for the transitions that are allowed in either the vibrational or intruder uncoupled, original basis) the correct behavior. There is the clear need, though, to carry out the full calculations in order to get the more detailed description of the E2 decay properties. A few cases remain where, even in the more detailed study, deviations are quite big, e.g. the $0_3^+ \rightarrow 2_1^+$ transition which is, in the calculation of Délèze [2], rather well reproduced. As discussed before, those small $B(E2)$ values result from destructive interference effects coming from the vibrational and intruder contributions (-23 and $+11$ $e\cdot\mathrm{fm}^2$ for the vibrational and intruder contributions, respectively, for the $0_3^+ \rightarrow 2_1^+$ E2 transition). Even tiny

Table 4
Detailed (full diagonalization) $B(E2;J_i^\pi \rightarrow J_f^\pi)$ values (in e^2fm^4 units) for ^{114}Cd. The data are compared with (i) the unperturbed $B(E2)$ values ($\alpha = \beta = 0$) and with the result of the full diagonalization ($U = U^{(w)}U^{(s)}$) ($\alpha = \beta = 0.08$). The values from Délèze et al. [2] [D] are also presented, for comparison

$J_i^\pi \rightarrow J_f^\pi$	Expt.	$\alpha = \beta = 0$	$\alpha = \beta = 0.08$	[D]
$2_1^+ \rightarrow 0_1^+$	1020	955	971	1152
$0_2^+ \rightarrow 2_1^+$	900	-	895	1394
$2_2^+ \rightarrow 0_1^+$	17	2.2	2.2	12
$\rightarrow 2_1^+$	724	1362	1373	1652
$\rightarrow 0_2^+$	60	-	14	116
$4_1^+ \rightarrow 2_1^+$	2020	1571	1623	1871
$\rightarrow 2_2^+$	136	41	3.7	22
$0_3^+ \rightarrow 2_1^+$	0.1	1091	314	0.6
$\rightarrow 2_2^+$	4476	762	1765	2452
$2_3^+ \rightarrow 0_1^+$	11	-	0.0	0.46
$\rightarrow 2_1^+$	1.3	-	50	20
$\rightarrow 0_2^+$	2167	3216	2134	1925
$\rightarrow 2_2^+$	1133	-	439	487
$\rightarrow 0_3^+$	230	-	811	823
$\rightarrow 4_1^+$	1533	-	604	770
$4_2^+ \rightarrow 2_1^+$	13	-	6.7	7.1
$\rightarrow 2_2^+$	1053	-	564	1678
$\rightarrow 2_3^+$	3785	4537	3420	642
$\rightarrow 4_1^+$	430	-	179	1031
$3_1^+ \rightarrow 2_1^+$	34–92		4.5	12
$\rightarrow 2_2^+$	1206–3200		1193	1707
$\rightarrow 4_1^+$	500–1400		410	656
$\rightarrow 2_3^+$	24–64		5.2	40
$\rightarrow 4_2^+$	<(340–930)		761	104
$0_4^+ \rightarrow 2_1^+$	190–490		4	16
$\rightarrow 2_3^+$	1400–3700		278	1189
$2_4^+ \rightarrow 0_1^+$	<1		0.1	10
$\rightarrow 2_1^+$	<5.8		10	2
$\rightarrow 0_2^+$	<280		68	74
$\rightarrow 2_2^+$	<38		12	67
$\rightarrow 0_3^+$	<240		1	1956
$\rightarrow 2_3^+$	<500		3335	1844
$6_1^+ \rightarrow 4_1^+$	3915	-	1825	2385
$6_2^+ \rightarrow 4_2^+$	4245	-	2701	3590

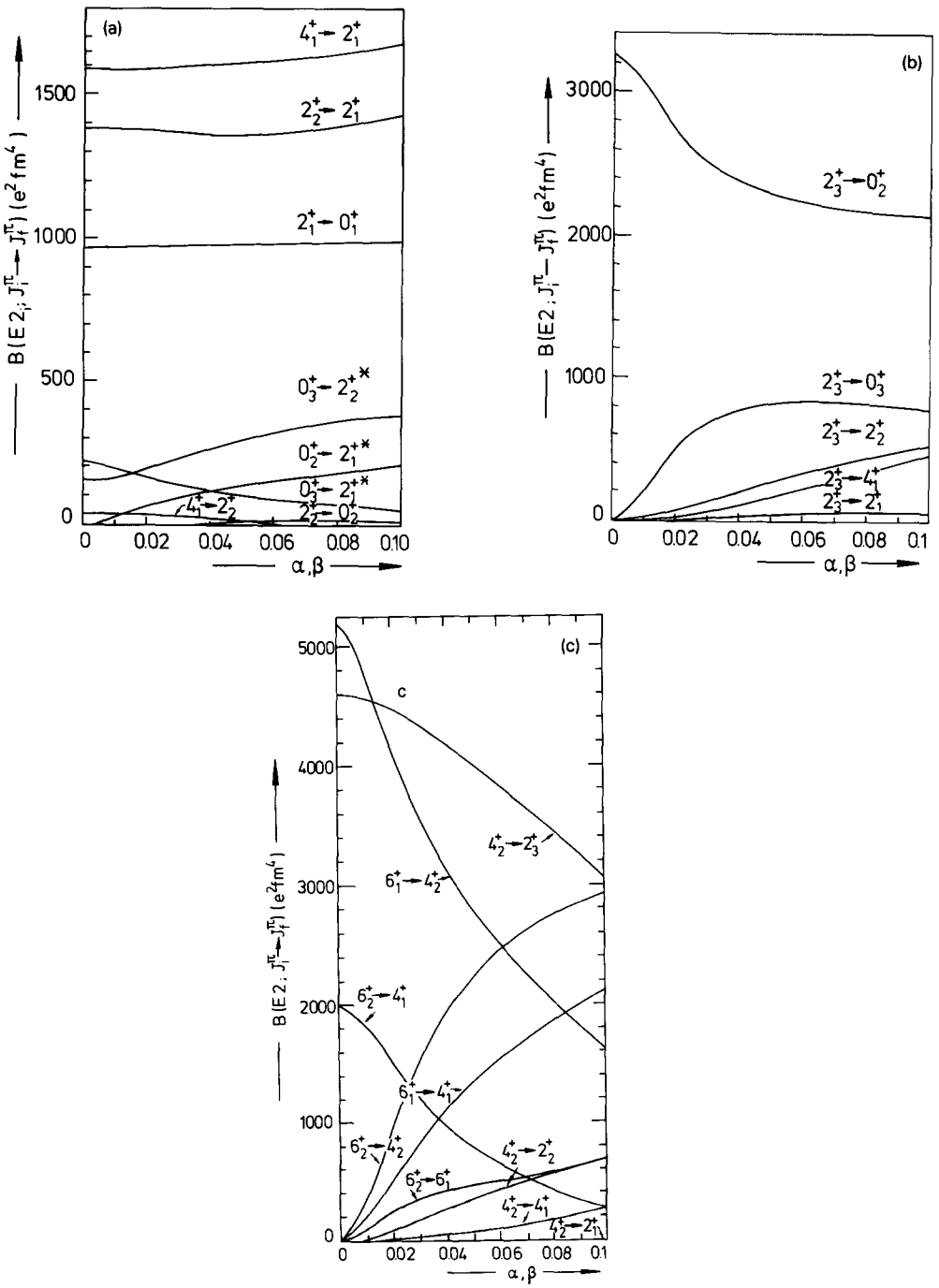

Fig. 7. (a)–(c) Variation of a number of $B(E2;J_i^\pi \rightarrow J_f^\pi)$ reduced E2 transition probabilities as a function of strengths α, β in the mixing hamiltonian of Eq. (5). The $B(E2)$ values marked with an asterisk (*) need to be multiplied by the statistical factor 5.

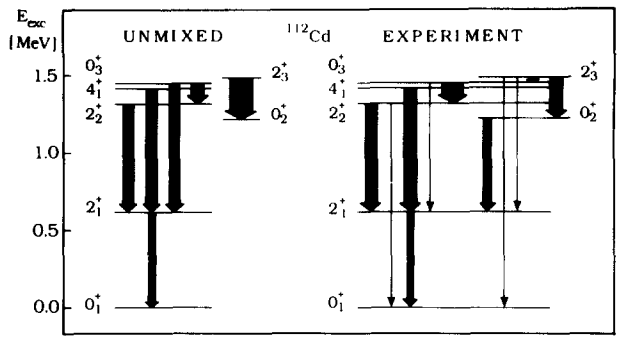

Fig. 8. The unmixed and experimental $B(E2)$ values for ^{112}Cd [19]. Same conventions as described in Figs. 5 and 6 are used.

changes in the hamiltonians (the difference between the calculations of Refs. [30] and [2], columns 4 and 5) can induce drastic changes and give an idea of the sensitivity of the model. Moreover, we observe that these $B(E2)$ values cannot be calculated in a *stable* way using the present approach. Since in these situations, we are concentrating on very small $B(E2)$ values, partly resulting from subtle interference effects, their exact reproduction is presently at the limit of applicability of the model.

Very similar results are obtained in $^{110,112}Cd$ and the unmixed and experimental situation are presented in Fig. 8 for ^{112}Cd, with mainly the same pattern as in ^{114}Cd, and as shown in recent studies [3,23,19,33], an even clearer presence of the O(5) symmetry shows up in this nucleus.

3. Conclusion

Results of low-spin gamma-ray spectroscopy, augmented by more selective reactions have made available level schemes that are (almost) complete in the even–even Cd nuclei up to $E_x \simeq 2.5$ MeV. Using both the energy spectra and the E2 transition rates, it has become possible to define the global structure in these nuclei as a combination of an anharmonic quadrupole vibrational spectrum (U(5)-like) and an intruder spectrum (more O(6)-like). This picture gives a fairly consistent description of most phenomena. Here, it has been shown that the concept of intruder analog multiplets can be used for the even–even Cd nuclei. Even though locally, in particular near the position of the two-quadrupole phonon 0^+, 2^+, 4^+ triplet, strong perturbations occur through mixing between the vibrational and intruder structures, the modification to the global structure remains moderate. A deeper insight in the coupling between the vibrational and intruder structure can be traced back to the analytical description of the U(5)–O(6) coupling model, as worked out in detail in Refs. [19,33]. Thus, shape or intruder state coexistence remains a valid picture to describe the even–even Cd-nuclei, in particular near the mid-shell $N = 66$ neutron region. We also have pointed out that by including the strong $0_2^+ - 0_3^+$ coupling in an intermediate step, an intermediate basis can be constructed such

that the difference between 2-phonon and intruder 0^+ states gets lost. This then gives rise to a very good new basis in order to understand the modifications thereby implied in the vibrational E2 intensity rules. This idea can give an indication why these nuclei seem to resemble a quadrupole vibrator with small perturbations in the E2 decay properties on one hand (a weak-mixing basis), while on the other hand the observed energy spectrum cannot be reconciled within an anharmonic vibrational description. Here, both the energies and E2 decay can be related with the "physical" basis obtained from the partial diagonalization i.e. $U^{(s)}\psi^{(0)}$, where $\psi^{(0)}$ denotes the original, zero-order basis.

Acknowledgements

The authors are grateful to P. Van Isacker, M. Délèze and R.F. Casten for many discussions on these intriguing facets of nuclear structure. Two of the authors (K.H. and C.D.C.) are grateful to the I.I.K.W. and N.F.W.O. for financial support. J.J. and H.L. acknowledge the support of the Swiss National Science Foundation. Part of this work was supported through the NATO research grant CRG 920011/R.

References

[1] J. Kern, A. Bruder, S. Drissi, V.A. Ionescu and D. Kusnezov, Nucl. Phys. A 512 (1990) 1.
[2] M. Délèze, S. Drissi, J. Kern, P.A. Tercier, J.P. Vorlet, J. Rikovska, T. Otsuka, S. Judge and A. Williams, Nucl. Phys. A 551 (1993) 269.
[3] M. Délèze, S. Drissi, J. Jolie, J. Kern and J.P. Vorlet, Nucl. Phys. 554 (1993) 1.
[4] J. Kumpulainen, R. Julin, J. Kantele, A. Passoja, W.H. Trzaska, E. Verho, J. Väärämäki, D. Cutoiu and M. Ivascu, Phys. Rev. C 45 (1992) 640.
[5] R.F. Casten, J. Jolie, H.G. Börner, D.S. Brenner, N.V. Zamfir, W.-T. Chou and A. Aprahamian, Phys. Lett. B 297 (1992) 19.
[6] C. Fahlander, A. Bäcklin, L. Hasselgren, A. Kavka, V. Mittal, L.E. Svensson, B. Varnestig, D. Cline, B. Kotlinski, H. Grein, E. Grosse, R. Kulessa, C. Michel, W. Spreng, H.J. Wollersheim and J. Stachel, Nucl. Phys. A 485 (1988) 327.
[7] A. Giannatiempo, A. Nannini, A. Perego, P. Sona and G. Maino, Phys. Rev. C 44 (1991) 1508.
[8] J. Wesseling, G.W. de Jager, H. de Vries, M.K. Harakeh, R. De Leo and M. Pignanelli, Phys. Lett. B 245 (1990) 338.
[9] J. Rikovska, N.J. Stone, P.M. Walker and W.B. Walters, Nucl. Phys. A 505 (1989) 145.
[10] J.L. Wood, K. Heyde, W. Nazarewicz, M. Huyse and P. Van Duppen, Phys. Reports 215 (1992) 101.
[11] K. Heyde, P. Van Isacker, M. Waroquier, J.L. Wood and R.A. Meyer, Phys. Reports 102 (1983) 291.
[12] P. Van Duppen, E. Coenen, K. Deneffe, M. Huyse, K. Heyde and P. Van Isacker, Phys. Rev. Lett. 52 (1984) 1974.
[13] P. Van Duppen, E. Coenen, K. Deneffe, M. Huyse and J.L. Wood, Phys. Rev. C 35 (1987) 1961.
[14] J. Bron et al., Nucl. Phys. A 318 (1979) 335.
[15] D.M. Brink, R. de Toleda Piza and A.K. Kerman, Phys. Lett. 19 (1965) 413.
[16] B. Sorensen, Phys. Lett. 21 (1966) 683.
[17] D.R. Bes and G.G. Dussel, Nucl. Phys. A 135 (1969) 1.
[18] F. Iachello and A. Arima, The interacting boson model (Cambridge Univ. Press, Cambridge, 1987).
[19] J. Jolie, in Proc. 8th Int. Conf. on Capture gamma-ray spectroscopy and related topics, ed. J. Kern (World Scientific, Singapore, 1994) p. 43;
H. Lehman, Diplomarbeit, Univ. de Fribourg (1994) unpublished.
[20] M. Piiparinen et al., Nucl. Phys. A 565 (1993) 671.

[21] I. Thorslund et al., Nucl. Phys. A 568 (1994) 306.
[22] D. Jerrestam et al., Nucl. Phys. A 571 (1994) 393.
[23] J. Jolie and H. Lehmann, Phys. Lett. B (in press).
[24] P.D. Duval and B.R. Barrett, Nucl. Phys. A 376 (1982) 213.
[25] M. Sambataro, Nucl. Phys. A 380 (1982) 365.
[26] K. Heyde, P. Van Isacker, M. Waroquier, G. Wenes and M. Sambataro, Phys. Rev. C 25 (1982) 3160.
[27] D. Kusnezov, A. Bruder, V. Ionescu, J. Kern, M. Rast, K. Heyde, P. Van Isacker, J. Moreau, M. Waroquier and R.A. Meyer, Helv. Phys. Acta 60 (1987) 456.
[28] A. Aprahamian, D.S. Brenner, R.F. Casten, R.L. Gill, A. Pitrowski and K. Heyde, Phys. Lett. B 140 (1984) 22.
[29] A. Mheemeed et al., Nucl. Phys. A 412 (1984) 113.
[30] J. Jolie and K. Heyde, Phys. Rev. C 42 (1990) 2034.
[31] K. Heyde, C. De Coster, J. Jolie and J.L. Wood, Phys. Rev. C 46 (1992) 541.
[32] K. Heyde, C. De Coster, J. Wood and J. Jolie, Phys. Rev. C 46 (1992) 2113.
[33] H. Lehmann and J. Jolie, to be published.
[34] M. Bertschy, S. Drissi, P.E. Garrett, J. Jolie, J. Kern, S. Mannanal, J.P. Vorlet, N. Warr and J. Suhonen, Phys. Rev. C (in press).
[35] R.F. Casten and D.D. Warner, Rev. Mod. Phys. 60 (1988) 389.
[36] R. Hertenberger et al., Nucl. Phys. A 574 (1994) 414.